

85.4 Gbit/s Real-Time OFDM Signal Generation with Transmission over 400 km and Preamble-less Reception

R. Schmogrow¹, R. Bouziane², D. Hillerkuss¹, P. A. Milder³, R. J. Koutsoyannis³, Y. Benlachtar², P. M. Watts², P. Bayvel², R. I. Killey², C. Koos¹, W. Freude¹, and J. Leuthold¹

1: Karlsruhe Institute of Technology (KIT), 76131 Karlsruhe, Germany

2: University College London, Optical Networks Group, Dept. Electronic and Electrical Engineering, London WC1E 7JE, UK

3: Carnegie Mellon University, Department of Electrical and Computer Engineering, Pittsburgh, PA 15213, USA

Author e-mail address: rene.schmogrow@kit.edu

Abstract: An optical real-time single-polarization OFDM transmitter encodes 85.4 Gbit/s onto 122 electrical subcarriers using 25 % cyclic prefix. A continuous synchronization process without using a preamble allows reception after 400 km SSMF.

OCIS codes: (060.4510) Optical communications; (060.1660) Coherent communications.

1. Introduction

Orthogonal frequency division multiplexing (OFDM) [1] has attracted major interest within the field of optical communications. While first experiments were based on offline processing, actual applications call for real-time signal processing. Recently, such OFDM transmitters (Tx) [2, 3] and receivers (Rx) [4] were demonstrated. For these experiments state-of-the-art field programmable gate arrays (FPGA) were employed.

In this paper we demonstrate a real-time OFDM transmitter using FPGAs that encode 85.4 Gbit/s on 122 electrical subcarriers (SC). To this end, a 128-point inverse fast Fourier transform (IFFT) based on the Spiral Generator [5] is employed. A cyclic prefix (CP) with a length of 25% of the symbol duration is added without the need for additional processing efforts like e. g. multiplexers or first-in first-out buffers (FIFO). This is done by changing the FPGA multi-gigabit Tx (MGT) registers from 32 bit to 40 bit and by adjusting the clock dividers on the Micram digital-to-analog converters (DAC), accordingly. The CP enables dispersion-tolerant transmission over up to 400 km of standard single mode fiber (SSMF). Four pilot tones help to perform frequency offset compensation and carrier phase recovery at the receiver, where data are processed offline. Here, a novel synchronization method is introduced for finding the optimum FFT window position without relying on a preamble (training symbols).

2. Experimental Setup

The experimental setup comprises a real-time OFDM Tx [5], a recirculating loop, and an Agilent N4391A optical modulation analyzer (OMA), Fig. 1(a). An optical I/Q-modulator encodes the real-time generated 28 GSa/s OFDM waveform onto an external cavity laser (ECL). The optical amplifiers in this setup are erbium-doped fiber amplifiers (EDFA). The amplified signal is fed to the recirculating loop, which comprises two amplified spans of 50 km SSMF, but no dispersion management. The signal is transmitted along with a holding beam provided by a distributed feedback laser (DFB) for keeping the EDFA at a nearly constant operating point. After a pre-determined number of roundtrips the signal is received by the OMA. A second ECL serves as local oscillator for the Rx.

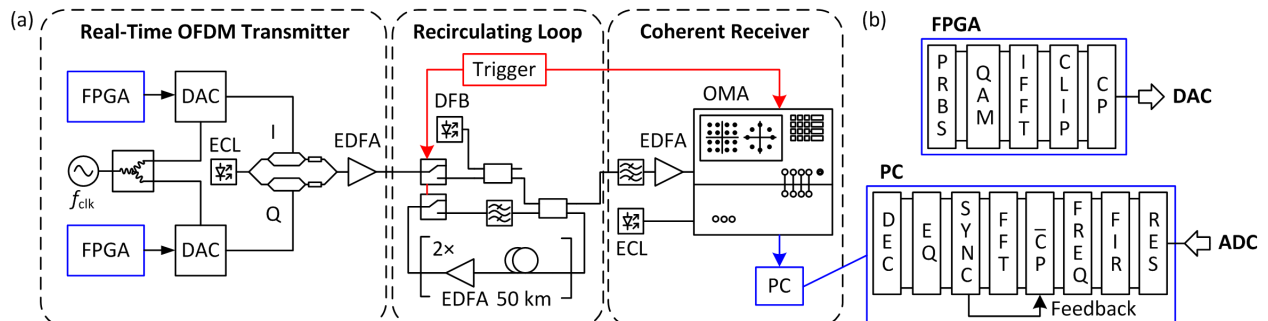


Fig. 1. Setup and DSP blocks of real-time OFDM Tx and offline OFDM Rx. (a) An FPGA based real-time Tx with optical I/Q-modulator and external cavity laser (ECL). The amplified signal is sent through a recirculating loop comprising two 50 km spans of SSMF with an EDFA. A DFB laser is used as a holding beam in the loop. A trigger source defines the amount of roundtrips by controlling optical switches and the OMA used to receive the signal. A second ECL serves as local oscillator. Data are processed on an external PC. (b) Real-time FPGA processing blocks comprising PRBS generation, 16QAM mapping, an IFFT, clipping, and cyclic prefix insertion. The offline processing blocks comprise resampling (RES), FIR filtering, frequency offset compensation (FREQ), cyclic prefix removal, an FFT, and a window synchronization module (SYNC), equalization (EQ), and decoding (DEC) of the data. The signal quality is evaluated through EVM measurements [6].

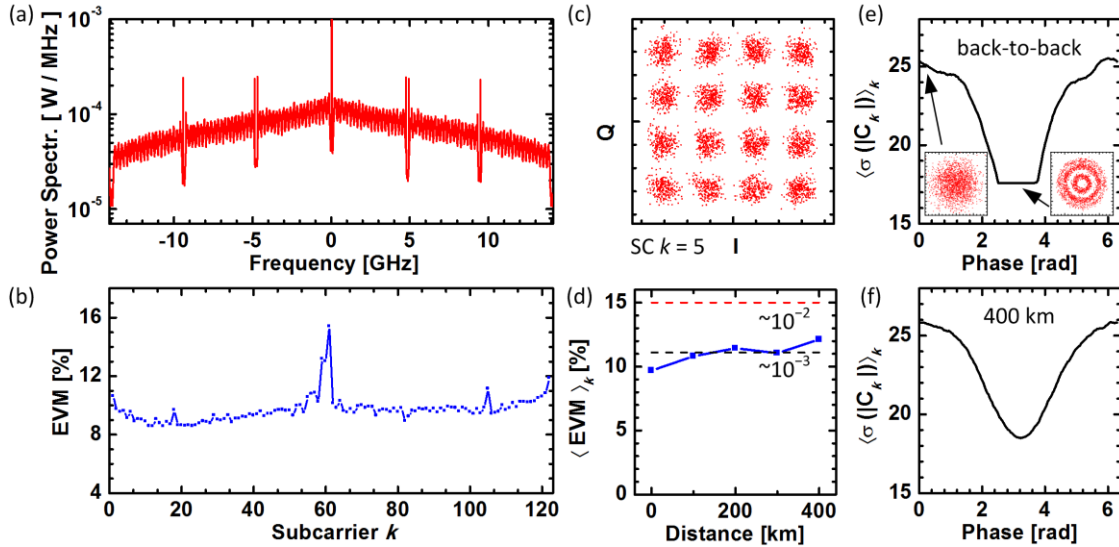


Fig. 2. Experimental results. (a) Measured and ensemble-averaged spectrum. Four pilot tones broadened by the CP are seen. (b) Signal quality, expressed by EVM [6] for different subcarrier positions k in a back-to-back measurement. (c) Constellation diagram of SC $k = 5$ and back-to-back configuration. (d) Average EVM for all SC after the transmission distance. FEC limits for BER of 10^{-3} and 10^{-2} are indicated. (e) Output of the FFT window synchronization module for back-to-back measurement. The optimum window position is found for the minimum mean value $\langle \sigma(|C_k|) \rangle_k$ of the standard deviation $\sigma(|C_k|)$ of subsequently received random modulation coefficients C_k in SC k , averaged over all SC k . The flat bottom of the “trough” is due to the phase tolerance introduced by the cyclic prefix. (f) Synchronization module output after 400 km transmission.

3. Processing Blocks and FFT Window Synchronization without Preamble

The real-time processing blocks implemented on the FPGA comprise pseudo random bit sequence generation (PRBS, $2^{15} - 1$), a 16QAM mapper, a 128-point IFFT core based on the Spiral Generator [5], clipping, and CP insertion, Fig. 1(b). For the offline decoding, standard OFDM processing blocks like finite impulse response (FIR) filtering, frequency offset compensation, CP removal, and an FFT are used. Common synchronization techniques for finding the correct temporal position of the FFT window rely on a preamble (training symbols). Here, we developed an alternative algorithm which we believe to be advantageous insofar, as the synchronization is a continuous process along with the reception. In contrast, using a preamble the system runs free between synchronization events. It is based on the observation that only for a synchronized FFT window the resulting constellation diagram exhibits some regularity (Fig. 2(e) right inset), while otherwise just an unstructured cloud of constellation points is observed (Fig. 2(e) left inset). As a measure of the constellation’s regularity we compute the standard deviation $\sigma(|C_k|)$ for the modulus of the complex set of randomly transmitted constellation points C_k for each SC k , and take average of σ over all SC, $\langle \sigma(|C_k|) \rangle_k$. For back-to-back operation, Fig. 2(e) shows the resulting averaged $\langle \sigma(|C_k|) \rangle_k$ as a function of the synchronization phase between Tx-IFFT and Rx-FFT window. The optimum phase is found in the region of the flat “trough” which is due to the window positioning tolerance introduced by the CP. This method can be applied prior to equalization as no phase or absolute amplitude information is required.

4. Results

The ensemble-averaged 28 GHz spectrum of the OFDM signal is shown in Fig. 2(a). Four pilot tones broadened by the CP can be seen. The roll-off stems from the frequency response of the system and is equalized in the Rx. The EVM performance [6] for each SC k is depicted in Fig. 2(b). A back-to-back received constellation diagram for SC $k = 5$ is shown in Fig. 2(c). Measurements have been done for several transmission distances. The average EVM over all 122 SC approaches the forward error correction (FEC) limits for bit error ratios (BER) of 10^{-3} and 10^{-2} as indicated in Fig. 2(d). The output of the FFT window synchronization module can be seen in Fig. 2(e) and (f). For back-to-back measurements suitable windows can be found within the range of the CP of 25 % of the symbol length, i. e., within $1 - (1 / 1.25) = 20\%$ (1.26 rad) of the maximum phase difference 2π . This is the trough width in Fig. 2(e). After transmission over 400 km of fiber the CP is fully needed for dispersion compensation. Therefore only a fixed FFT window position at the minimum $\langle \sigma(|C_k|) \rangle_k$ offers best performance.

5. References

- [1] W. Shieh et al., Opt. Express **16**, 841-859 (2008).
- [2] B. Inan et al., OFC 2011 paper OMS2.
- [3] R. Schmogrow et al., Opt. Express **19**, 12740-12749 (2011).
- [4] N. Kaneda et al., JLT **28**, pp. 494-501 (2010).
- [5] Y. Benlachtar et al., IEEE J SEL TOP QUANT **16**, 5, pp. 1235-1244.
- [6] R. Schmogrow et al., PTL, doi: [10.1109/LPT.2011.2172405](https://doi.org/10.1109/LPT.2011.2172405).